

Atomistic Insights into the Nanofluid Transport through Ultra-confined Capillary

Xiao Wang ¹, Zhiliang Zhang ¹, Ole Torsæter ^{2,3}, and Jianying He ^{1,*}

¹ NTNU Nanomechanical Lab, Department of Structural Engineering, Faculty of Engineering, Norwegian University of Science and Technology (NTNU), 7491 Trondheim, Norway

² Department of Geoscience and Petroleum, Faculty of Engineering, Norwegian University of Science and Technology (NTNU), 7491 Trondheim, Norway

³ PoreLab, Norwegian University of Science and Technology (NTNU), 7491 Trondheim, Norway

* Corresponding author:

Jianying He

Email: jianying.he@ntnu.no

Tel.: +47-73594686

Abstract:

The nanofluids or nanoparticles (NPs) transport in confined channel is of great importance for many biological and industrial processes. In this study, molecular dynamics simulation has been employed to investigate spontaneous two-phase displacement process in ultra-confined capillary controlled by surface wettability of NPs. The results clearly show that the presence of NPs modulates the fluid-fluid meniscus and hinders displacement process compared with NP-free case. From the perspective of motion behavior, hydrophilic NPs disperse in water phase or adsorb on the capillary, while hydrophobic and mixed-wet NPs are mainly distributed in the fluid phase. The NPs dispersed into fluids tend to increase the viscosity of fluids, while the adsorbed NPs contribute to wettability alteration of solid capillary. Via capillary number calculation, it is uncovered that the viscosity increase of fluids is responsible for hindered spontaneous displacement process by hydrophobic and mixed NPs. Wettability alteration of capillary induced by adsorbed NPs is dominating the enhanced displacement in the case of hydrophilic NPs. Our findings provide the guidance to modify the rate of capillary filling and reveal microscopic mechanism of transporting NPs into porous media, which is significant to the design of NPs for target applications.

Keywords: Two-phase displacement; Surface wettability of nanoparticles; Molecular dynamics simulation;

1. Introduction

The displacement of multiphase flow through micro or nanoscopic channel is of broad interest in many natural and industrial processes, such as ink jet printing, drug delivery^{1, 2}, oil field³, nanofluidic^{4, 5}, etc. Two parameters are very crucial to the displacement process, the velocity of displacing phase⁶⁻⁸ and displacement efficiency in the capillary⁹⁻¹¹. For example, in ink jet printing the drying time and clarity of printed image are closely related to the rate of capillary filling. The target in enhanced oil recovery (EOR) is to extract more trapped crude oil from reservoir channels. Therefore, the fundamental understanding of the displacement mechanism is of high importance and calls for research effort.

The common feature on two-phase displacement is that the nonaqueous phase, which does not dissolve in or easily mix with water, is displaced by the other aqueous displacing liquids. The contact angle θ ^{8, 12}, interfacial tension γ and viscosity η ¹³ are key properties controlling the transport of complex fluids into nanopores. Usually, some chemical additives^{2, 14, 15}, such as surfactants^{16, 17} or polymers are added into aqueous fluids to adjust these parameters. One of the emerging interests is the new generation fluids called nanofluids, a class of fluids engineered by dispersing nanoparticles (NPs) in base fluids, which were first known as its thermal properties^{18, 19}.

In the past decades, a renewed interest arises in the application of nanofluids for enhanced oil recovery²⁰⁻²², such as changing the viscosity of fluids²³, reducing interfacial tension, altering the rock surface wettability^{21, 24}, and increasing the mobility of the capillary-trapped nonaqueous phase. In the year of 2003, Wasan and Nikolov²⁵ proposed that NPs self-assembled and formed two-dimensional (2-D) layered structures in the three-phase (solid–oil–aqueous phase) contact region, producing a structural disjoining pressure and thus promoting detachment of oil droplets from solid surface. Since then, many experiments were performed to validate and explain the mechanism of NPs for EOR²⁶. Hu et al.²⁷ reported a study of TiO₂

NP-assisted brine flooding for oil recovery, and proposed the mechanisms, including improvement of mobility ratio, wettability alteration of capillary, etc. Although some progresses on NPs for EOR have been reported recently^{20, 28, 29}, the displacement mechanisms of nanofluids in porous media are still not understood. Wasan et al.³⁰ found that when sodium dodecyl sulfate micellar solution was injected into glass capillaries, hexadecane formed spherical drops and was detached from the capillary surface. These experimental investigations facilitate the understanding on how the oil films are extracted from porous media. However, it is very challenging to control the thickness of oil film in experiments, the accurate size of NPs, the nanoscale diameter of capillary, etc., and therefore is difficult to disentangle the specific roles of various interfaces in two-phase displacement.

Molecular dynamics simulation has great potentials to gain microscopic insights into the displacement process, including motion behavior of molecules and tuning specific parameters, complementary to experimental observations³¹⁻³⁴. Numerous simulations have been carried out to study capillary filling of single-component fluids into nanochannels with varying geometries^{35, 36}, and two-phase displacement process as well. Chen et al.³⁷ investigated spontaneous and forced water-oil displacement in capillary by dissipative particle dynamics (DPD). Their simulations concluded that tuning the surface wettability of solid and weakening the external force were possible to extract entire trapped oil from channel. Until now, the transport of nanofluids into porous media or nanochannel are sparsely studied by atomic or molecular simulation.

The purpose of this work is to explore the water-oil displacement mechanism by modulating surface wettability of NPs in molecular dynamic simulation, and identify the dominating driving force for spontaneous capillary displacement process into porous media. The relationship between displacement length (l) vs time (t), and interfacial thickness is analyzed to study the displacement process quantitatively. Moreover, dynamic behavior of NPs

is captured and capillary number is calculated to reveal the involved mechanism responsible for flow behavior. Our findings provide guidance to modify the macroscopic behavior of two-phase displacement, such as, controlling the velocity of fluids and designing suitable NPs for EOR or other relevant applications.

2. Model and Simulation Details

2.1 Model systems

Our goal is to model the two-phase displacement process in a nanochannel. A single cylindrical capillary is constructed to mimic micro model in porous media^{10, 38}. The system is shown in Figure 1, containing a water-based fluid with dispersed spherical NPs as displacing phase, oil as displaced phase and capillary.

The solid cylindrical capillary with radius $R = 25 \text{ \AA}$ was constructed from a silicon block with cross-sectional dimensions $x = z = 65.1684 \text{ \AA}$ and the axial length $y = 194.1475 \text{ \AA}$, by removing all the atoms lying along the axial direction. Displacing phase was consisted of 20,000 water molecules and 16 spherical NPs with a diameter of 7.0 \AA well-distributed in water phase. So the volume fraction of NPs was approximately 4.0%^{28, 39, 40}. A cylindrical oil model composed by decane⁴¹ molecules within the radius of $\sim 20 \text{ \AA}$ was built as displaced phase to fully fill cylindrical capillary. An equilibrium calculation was carried out for 1.0 ns to obtain a steady-state distribution of oil in the capillary.

Hydrophobic, mixed-wet, and hydrophilic NPs were applied in the water-oil displacement process to explore the migration mechanism of nanofluids into porous media. All the simulations were conducted in a periodic orthorhombic box, and a vacuum was constructed along the y direction to eliminate the boundary effect⁴².

2.2 Computational Details

LAMMPS package⁴³ was employed to carry out all the simulations. During simulations, water molecules were described by the simple point charge/extend SPC/E model⁴⁴, and oil

molecules were modeled by the CHARMM force field^{45,46}. The well-known standard pairwise 12-6 Lennard-Jones (L-J) potential was employed to describe nonbonded intermolecular atom-atom interactions, as stated in Equation (1). The long range coulomb interaction was described by Equation (2).

$$U_{LJ} = 4\epsilon_{ij} \left[\left(\frac{\sigma_{ij}}{r_{ij}} \right)^{12} - \left(\frac{\sigma_{ij}}{r_{ij}} \right)^6 \right] \quad (1)$$

$$U_{coulomb} = \frac{q_i q_j}{4\pi\epsilon_0 r_{ij}} \quad (2)$$

where ϵ_{ij} and σ_{ij} represented the LJ potential well depth and zero potential distance, and r_{ij} was the distance between atom i and j . The q_i and q_j were charges on atom i and j , and ϵ_0 was the vacuum permittivity. The Lorentz-Berthelot mixing rule, $\sigma_{ij} = (\sigma_i + \sigma_j)/2$ and $\epsilon_{ij} = \sqrt{\epsilon_i \cdot \epsilon_j}$, was employed to average the parameters for the interactions between oil-water, water-capillary and oil-capillary.

In our simulation, the main purpose is to study the effect of surface wettability of NPs in a wide range, rather than to demonstrate a specific material. If a certain atom type was specified, its LJ interaction with liquid is always a fixed value, and inappropriate for adjusting the surface wettability^{40,47}. Thereby, materials for capillary and NPs were not specified in our work. Surface wettability of capillary and NPs was tuned by varying characteristic energy well depth ϵ_{ij} in an appropriate range. In order to trigger spontaneous displacement, the inner surface of capillary must have stronger tendency to water than oil molecules. The detailed information about the selection of characteristic energy for capillary was given in Supporting Information S1. Accordingly, the characteristic energy between capillary and water ϵ_{wo} was chosen to be 0.6 kcal/mol, which meant a hydrophilic capillary.

The main characteristic energies for NPs are interactions with water ϵ_{nw} and NP-NP ϵ_{nn} . The characteristic energy for NP-NP ϵ_{nn} was set relatively small for a weak interaction between

NPs. By tuning characteristic energy ε_{nw} between NPs and water, NPs with diverse wettability were obtained. The detailed forced field parameters were listed in Supporting Information S2. Atoms in both NPs and the capillary were charge free.

All the systems were first energy-minimized with steepest descent method, followed by simulations performed under NVT ensemble (constant number of particles, volume, and temperature). During MD simulation process, Nosé–Hoover thermostat⁴⁸ was employed to keep constant temperature of 298 K with 1.0 ps damping coefficient. The Velocity Verlet algorithm was used to integrate Newton’s motion equation. The cut off was 1.0 nm for Lennard-Jones nonbonded potential, and the long range electrostatics interaction was compensated by using the particle–particle–particle–mesh (PPPM) algorithm⁴⁹, with a convergence parameter of 10^{-4} . NPs always moved and rotated as a single entity, ignoring internal interaction. Meanwhile, atoms in the solid capillary were fixed to reduce simulation time. It took 16 ns for NP-free system to displace oil molecules out of the capillary, and thus the total simulation time for all systems was chosen to be 16 ns for comparison, with a time step of 1 fs. The configurations were viewed by VMD software⁵⁰.

3. Results and Discussion

3.1 Spontaneous capillary displacement process

3.1.1 Displacement phenomena

Water-oil displacement process is displayed in Figure 2 to intuitively observe the dynamic behavior of fluids with different surface wettability of NPs. For base fluid without NPs, while water starts to flow into capillary with concave meniscus, some oil molecules are displaced out from the capillary. When increasing to 16 ns, almost all the oil molecules are displaced. Compared with water fluid, the addition of NPs influences not only the meniscus but also the speed of spontaneous displacement process. Hydrophilic NPs are still well dispersed in water phase, and the nanofluid displaces all the oil molecules at 16 ns, while the meniscus is slightly

changed compared with NP-free case. In the case of the mixed and hydrophobic NPs, it is interesting to see that some NPs move into the oil phase, and there is still some oil left in the capillary at 16 ns.

The density distribution profiles of displacing fluids along axial direction is calculated, taking the one for base fluid as an example in Figure 3. The density for water in the capillary is about 0.95 g/cm^3 , comparable with the experimental value of 1.0 g/cm^3 . As the time increases, the density for water along the axial direction keeps stable, demonstrating the incompressible and stable flow properties in our simulations. Based on density profiles, the migrating distance of displacing phase into capillary is at the location where the fluid density reaches 50% of its bulk value, which is also considered as the liquid–liquid interface. Therefore, the quantitative information about dynamic displacement process can be obtained from the resulting motion curves.

The relation between displacement length of fluids into capillary (l) and time (t) is plotted in Figure 4. The displacement length l for water and nanofluids in capillary obeys the relationship of \sqrt{t} , similar to the previous study⁴⁰. In order to examine the displacement processes in detail, the patterns labeled with various colors are enlarged in Figure 4(b). At the beginning of displacement process from 0.0 to ~ 1.2 ns in Figure 4(b)I, there is no obvious difference in all the fluids. With the time increase to 4 ns, displacement of all the nanofluids is slightly higher than the NP-free case (Figure 4(b)II). However, when further increasing to 10.0 ns, displacement for mixed and hydrophobic NPs becomes lower than that for hydrophilic NPs and water systems, as shown in Figure 4(b)III. The displacement has a relative reduction for mixed and hydrophobic NPs, indicating that the water-oil displacement process is inhibited with the addition of these types NPs.

3.1.2 Interfacial thickness

Interfacial properties of fluid-fluid can reveal the fundamental mechanisms underlying spontaneous displacement process, for example, the shape of meniscus is determined by the wetting property of the capillary and the displacement dynamics. One of the key properties is interfacial thickness, which is closely related to three-phase contact angle and interfacial tension of fluids. The dynamic interfacial thickness is analyzed to characterize the interfacial change and NP effect during the displacement process, as shown in Figure 5.

The interfacial thickness for two fluids is calculated by the “90-90” criterion⁵¹, defined as positions where the densities of two phases locate at 90% of their bulk value (the light blue region depicted in Figure 5(a)). The dynamic interfacial thickness for all kinds of NPs is summarized in Figure 5(b). Here, three typical stages are identified for the spontaneous capillary displacement process, i.e. Developing Stage, Transition Stage and Equilibrium Stage, respectively. The Developing Stage ranges from $t=0$ to $t\sim 1.2$ ns, which is the acceleration process for fluids in the capillary. In this stage, the water molecules enter into the capillary and start to contact with oil phase, resulting in a sudden increase of interfacial thickness for all types of fluids. The meniscus at water-oil interface is developing at this stage. Spontaneous displacement process is mainly induced by water fluids, and therefore the effect of NPs on fluid displacement is negligible, as seen in Figure 4(b)I. The Transition Stage ranges from 1.2 ns to approximate 10.0 ns. The mixture of displacing fluids and oil is completed and a stable meniscus forms. As a result, interfacial thickness tends to a dynamic equilibrium although some fluctuations take place for nanofluids. Finally, interfacial thickness for all the systems reaches almost same dynamic equilibrium value in the Equilibrium Stage. Therefore, the influence of NPs wettability mainly acts in the Transition Stage. During the whole Transition Stage, the interfacial thickness of fluids with hydrophilic NPs is slightly smaller than that of NP-free system, while interfacial thickness for hydrophobic NPs has a largest fluctuation and tends to

be stable due to re-distribution of NPs. The curve for mixed NPs fluid almost coincides with the black curve in Figure 5(b), which suggests the similar behavior with NP-free case.

Interfacial thickness is closely related to interfacial tension and three-phase contact angle. Generally, the thicker the interfacial thickness, the lower the interfacial tension⁵². Therefore, the interfacial tension for the fluid with hydrophilic NPs slightly increases and then decreases in the Transition Stage, and reaches a similar dynamic equilibrium in Equilibrium Stage compared with that for the base fluid. For hydrophobic NPs, the interfacial tension first decreases in the Transition Stage and then increases to dynamic equilibrium value as the transportation of NPs from water to oil phase. The trend of dynamic interfacial tension for mixed NPs is almost the same for NP-free system. As there is a positive relationship between interfacial tension and displacement⁵³, the displacement behavior in Figure 4(b)II is attributed to the interfacial tension modified by NPs. However, no matter what kind of NPs, the equilibrium value of interfacial tension is similar with the base fluid at the Equilibrium Stage. Thus, the interfacial tension mainly acts in the Transition Stage, and is the secondary rather than dominating parameter during displacement process for nanofluids.

3.2 Mechanism of Spontaneous capillary displacement phenomenon

Above results indicate that parameters in addition to the interfacial tension should be explored with regard to the role of NPs played in the displacement mechanism. Our previous study⁴⁰ has revealed that properties of fluids is close linked with dynamic motion of NPs. Therefore, the motion behavior of NPs is analyzed to clarify the mechanism of displacement influenced by wetting properties of NPs in the following.

3.2.1 Micro behavior of nanoparticles

In Figure 2, four motion behaviors can be observed for diverse NPs, i.e. NPs dispersed in water phase, NPs dispersed in oil phase, NPs adsorbed on interface of fluid-fluid, and NPs adsorbed on solid capillary. The number of NPs with four motion behaviors is summarized in

Table 1, where the fraction number shows how many NPs aggregated into bigger ones, i.e. 2/9 means 9 NPs aggregate into 2 clusters.

As depicted in Table 1, at beginning of the simulation, most of NPs are dispersed in water phase for all nanofluids, though hydrophobic NPs intend to agglomerate. With the time increasing from 2.0 ns to 14.0 ns, the number of hydrophilic NPs in water phase decreases to nine, and only one NP stays stably at fluid-fluid interface, while the rest are adsorbed onto solid capillary. For fluids with mixed NPs, after 14.0 ns simulation, six NPs are dispersed in water and oil phase separately, only one is trapped at fluid-fluid interface and three are adsorbed on solid capillary. For hydrophobic NPs, initially, about two particles stay at interface and then decrease to none before 10.0 ns, resulting in the change of interfacial thickness, in agreement with the Transition Stage shown in Figure 5(b). With the time evolution, hydrophobic NPs tend to move into oil phase, and the rest of NPs left in water phase aggregates into bigger clusters. Hence, hydrophilic NPs are either dispersed in water phase or adsorbed on solid capillary, while hydrophobic and mixed NPs are mainly dispersed in liquid phase. The influence of these two behaviors on the properties of fluid, such as viscosity and wettability of capillary, will be discussed in the following section.

3.2.2 NPs dispersed in liquid phase

The NPs dispersed into liquid phase have an impact on the rearrangement of liquids molecules, and thence result in the variant diffusion behavior and properties of fluids. Here, a simple model^{39, 40} consisted of NP and water or oil molecules was constructed to study the influence of dispersed NPs, and the same characteristic energy parameters were selected as described in Section 2. The mean square displacement (MSD) curves of water or oil are plotted in Figure 6 to evaluate the influence of NPs with varied surface wettability. When the NPs in the water phase alter from hydrophobic to hydrophilic, the diffusion of water molecules decelerates owing to the stronger interaction between hydrophilic NPs and water molecules.

Similarly, in the oil phase, hydrophobic NPs induce the slower movement of oil molecules, while hydrophilic NPs tend to escape from oil phase and have minor effect on the diffusion of oil phase. Generally, the diffusion of liquid has an inverse relation with viscosity ⁶, i.e. the quicker liquid moves, the lower viscosity it has. Therefore, the hydrophilic NPs have potential to increase the viscosity of water, while hydrophobic NPs dispersed in oil phase lead to higher viscosity of oil.

The interaction energy between NPs and fluid is calculated to explore the potential mechanism of viscosity variation due to the dispersed NPs (shown in Figure S3 in Supporting information). It is foreseen that hydrophilic NPs have stronger interaction with the water phase, while hydrophobic ones have stronger interaction with oil molecules. According to our previous results ⁴⁰, higher interaction energy leads to more liquid molecules adsorbed onto NPs, and then move together as an entirety in the capillary. This type of configuration largely limits the diffusion of liquid molecules, resulting in increase of viscosity. Thus, the increased viscosity of liquid phase can be attributed to the improved interaction between dispersed NPs and liquid molecules.

According to the Lucas-Washburn equation and other theoretical models about imbibition and displacement process³⁷, there is an inverse relation between viscosity and imbibition length in the capillary. Hence, NP-induced increase in viscosity will inhibit the fluid displacement in capillary, and this is the main reason why fluids with mixed and hydrophobic NPs have smaller displacement compared with NP-free and hydrophilic NPs cases.

3.2.3 NPs adsorbed on the capillary

In the case of hydrophilic NPs, about half of NPs adsorb onto the wall of the capillary during displacement process, as shown in Table 1. The previous simulation ⁴⁰ about MSD of hydrophilic NPs in the capillary along the axial direction indicates that the adsorbed hydrophilic NPs stick onto capillary strongly, facilitating the wettability alteration of the solid

capillary and hence promoting the displacement process of fluids. Meanwhile, due to the immobile molecules at nanochannel wall, the sticking adsorbed hydrophilic NPs also has potential to result in a reduced effective hydraulic diameter of the channels and transport rate^{54, 55}.

To further validate the influence of adsorbed NPs on displacement process, another system considering very low interaction energy between NPs and solid capillary ($\varepsilon_{ns}=0.2$ kcal/mol) was simulated, while all other parameters were the same as described in Section 2. Comparing two sets of snapshots in Figure 7, lower interaction energy induces less NPs adsorbing onto the wall of the capillary. A water layer always exists between NP and the capillary, which is attributed to the competitive adsorption between NPs and water molecules. Water molecules have higher adsorption strength to the capillary than NPs, thus leading to the existence of water layer. After 16.0 ns simulation, there are still oil molecules left in the capillary, meaning a slower displacement velocity for fluids with $\varepsilon_{ns}=0.2$ kcal/mol. This further confirms that the adsorbed NPs on capillary improve the displacement velocity in our system.

It can be summarized that even though the dispersed hydrophilic NPs in liquids tends to retard displacement process, the hydrophilic NPs adsorbed on the capillary facilitate the displacement process. This explains why displacement for fluids with hydrophilic NPs is quicker than other nanofluids.

3.3 Comparison between Capillary force and Viscous force

One of the proposed microscopic mechanisms for displacement process is that the addition of NPs modifies the capillary force and viscous force^{27, 56}, resulting in the different displacement velocity and efficiency. In order to assess the dominating effect of capillary or viscous force on spontaneous displacement process, a dimensionless parameter called capillary number is adopted²⁷.

$$N_c = \frac{\eta_{inj} \times \nu}{\sigma_{ow}} \quad (3)$$

where η_{inj} is the viscosity of injected liquid (Pa·s), ν is the flow velocity (m/s) and σ_{ow} is the interfacial tension of water-oil interface. For ordinary water-flooding conditions, the capillary force is predominant if the order of capillary number is in the range of $<10^{-5(4)}$. When the capillary number exceeds a value of 10^{-4} , the viscous force will have a great effect on the displacement process, and the oil phase or non-wetting phase becomes relatively easier to be extracted from the capillary or pores ⁵⁶.

Here, the water-oil system without NPs is taken as an example to calculate capillary number. Initially, the interfacial tension of water-oil, viscosity of water fluids, and displacing velocity of water phase are calculated, respectively. For interfacial tension, the detailed model and parameters are listed in Supporting Information S4. The interfacial tension of water-oil is derived by subtracting mean tangential stress tensors (i.e., P_{xx} and P_{yy}) from the normal one (i.e., P_{zz}) ⁵⁷.

$$\sigma_{wo} = \frac{1}{2} L_z \left\langle P_{zz} - \frac{1}{2} (P_{xx} + P_{yy}) \right\rangle \quad (4)$$

where L_z is the length of simulation box in z axis. The calculated interfacial tension for decane/water interface is 50.54 ± 1.28 mN/m, in good agreement with the experimental value of 51.98 mN/m⁵⁸.

The method described in section 3.2.2 is used to calculate viscosity of water phase. The viscosity of nanofluid η is derived by importing the Einstein relation ⁶.

$$\eta = \frac{k_B T}{3\pi r_w} \frac{1}{D} \quad (5)$$

where k_B is the Boltzmann constant, T is simulation temperature, and r_w is the molecular diameter, which is set to be 0.17 nm⁶. Based on the MSD curves, the self-diffusion coefficient D for water is calculated by the following equation:

$$D = \frac{1}{6} \lim_{t \rightarrow \infty} \frac{d}{dt} \sum_i^n \langle |R_i(t) - R_i(0)|^2 \rangle \quad (6)$$

where $R_i(t)$ and $R_i(0)$ are the positions of atoms i at time t and 0, respectively, and $|R_i(t) - R_i(0)|^2$ is the mean square displacement (MSD).

According to MSD curve for water (Supporting Information S5), the calculated self-diffusion coefficient is $2.67 \times 10^{-9} \text{m}^2 \text{s}^{-1}$, which matches well with experimental data (2.09 - $2.66 \times 10^{-9} \text{m}^2 \text{s}^{-1}$) and other simulation results⁵⁹. The calculated viscosity of water is 0.9622 MPa·s under 298.15 K using Eq.5, in good agreement with experimentally measured value of 1.0 MPa·s.

Furthermore, the velocity for water-oil displacement into capillary is calculated approximately by linearly fitting the $l(t)$ curve in Figure 4 after the developing region ~ 1.2 ns. The calculated velocity is about 1.0 m/s for water fluids into the capillary spontaneously.

As values for all the parameters in Eq.3 are already known, the magnitude of capillary number is estimated to be 10^{-2} , which is much higher than the order of $10^{-5(4)}$ for ordinary water-flooding in reservoir condition^{27, 56}. Such high order of capillary number can be ascribed as the ultra-confined capillary, and indicates that the viscous force is significant in our displacement process, which also validates our previous analyses. Meanwhile, according to previous experimental studies, when the order of capillary number reaches 10^{-2} , there is almost no residual oil or non-aqueous displaced phase left in nanochannel and the recovery rate reaches almost 100%⁵⁶. In our cases, the same phenomenon that all the oil molecules have been displaced from the capillary is observed, as shown in Figure 2.

Therefore, viscous force of fluids is susceptible to the addition of NPs. For hydrophilic NPs, the dispersed NPs reduce the motion of water molecules, leading to the enhancement of water viscosity and thus the retarded displacement process. However, the majority of hydrophilic NPs adsorbs onto the wall of capillary, which has the potential to alter the wettability of solid capillary and improve the displacement process. Both the capillary force and viscous force are tuned simultaneously by hydrophilic NPs compared with NP-free and other NPs fluids. For the case with mixed NPs, some remain in the water phase, and some transport and disperse into the oil phase, modifying the viscous forces of displacing and displaced phase simultaneously. For the hydrophobic NPs, almost all the NPs move into oil phase and the enhanced viscous force of displaced phase plays a main role to hinder the displacement.

4. Conclusions

Herein, we employed molecular dynamics simulation to study the influence of surface wettability of NPs on the water-oil displacement process. It is found that spontaneous displacement l for fluids into the capillary scales with the square root of time, \sqrt{t} . All curves keep the similar tendency for the displacing fluids, and the displacement velocity varied with surface wettability of nanoparticles. Interfacial thickness analyses indicate that all fluids undergo three stages: Developing Stage, Transition Stage and Equilibrium Stage during the displacement process. Interfacial tension mainly acts during the Transition Stage, indicating the secondary rather than the dominating parameter in displacement processes of nanofluids.

Motion behavior of hydrophilic NPs reveals that dispersed NPs increase the viscosity of water while the adsorbed NPs contribute to the wettability alteration of capillary. For mixed NPs, almost half of NPs stay into the water phase, and the rest mainly disperse in oil phase. Hydrophobic NPs tend to transport into oil phase, otherwise aggregate into bigger clusters. The

increased viscosity of displaced phase by mixed and hydrophobic retard the displacement process, playing a key role in the Equilibrium Stage.

Finally, capillary number is calculated to identify the relative importance of viscous force and capillary force. Both forces are changed simultaneously by hydrophilic NPs, while only viscous force is responsible for displacement controlled by hydrophobic and mixed NPs. Our findings provide the guidance for modifying the rate of filling by different NPs and designing suitable nanoparticles for applications to number of technologies, including enhanced oil recovery.

Supplementary Materials: The following are available online at <http://>.

Acknowledgments: This work is supported by the Research Council of Norway, Aker BP ASA, and Wintershall Norge AS via WINPA project (NANO2021 and PETROMAKSII 234626). The computational resources are provided by Norwegian Metacenter for Computational Science (NOTUR NN9110k and NN9391k).

Conflicts of Interest: The authors declare no conflict of interest.

References

1. P. Kral and B. Wang, *Chem. Rev.*, 2013, **113**, 3372-3390.
2. I. C. Chen, M. Zhang, B. Teipel, I. S. de Araujo, Y. Yegin and M. Akbulut, *Environ. Sci. Technol.*, 2015, **49**, 3575-3583.
3. K. Y. Yoon, H. A. Son, S. K. Choi, J. W. Kim, W. M. Sung and H. T. Kim, *Energy & Fuels*, 2016, **30**, 2628-2635.
4. R. Devendra and G. Drazer, *Anal Chem*, 2012, **84**, 10621-10627.
5. A. R. Koltonow and J. Huang, *Science*, 2016, **351**, 1395.
6. J. A. Thomas and A. J. H. McGaughey, *Nano Lett*, 2008, **8**, 2788-2793.
7. W. Li, W. Wang, X. Zheng, Z. Dong, Y. Yan and J. Zhang, *Comput. Mater. Sci.*, 2017, **136**, 60-66.
8. K. Wu, Z. Chen, J. Li, X. Li, J. Xua and X. Dong, *Proc. Nat. Acad. Sci. U.S.A.*, 2017, **114**, 3358-3363.
9. H. Yan and S. Yuan, *J. Phys. Chem. C.*, 2016, **120**, 2667-2674.
10. T. Lee, L. Bocquet and B. Coasne, *Nat Commun*, 2016, **7**, 11890.
11. H. Zhang, T. S. Ramakrishnan, A. Nikolov and D. Wasan, *Energy & Fuels*, 2016, **30**, 2771-2779.
12. F. Jiménez-Ángeles and A. Firoozabadi, *J. Phys. Chem. C.*, 2016, **120**, 24688-24696.
13. Y. Kobayashi and N. Arai, *Langmuir*, 2017, **33**, 736-743.
14. A. J. Pak and G. S. Hwang, *J. Phys. Chem. C.*, 2016, **120**, 24560-24567.
15. M. J. Alshakhs and A. R. Kavscek, *Adv. Colloid Interface Sci.*, 2016, **233**, 126-138.
16. P. S. Hammond and E. Unsal, *Langmuir*, 2009, **25**, 12591-12603.
17. P. D. Fletcher, L. D. Savory, F. Woods, A. Clarke and A. M. Howe, *Langmuir*, 2015, **31**, 3076-3085.
18. A. Mohebbi, *J. Mol. Liq.*, 2012, **175**, 51-58.
19. Y. Ma, A. Bhattacharya, O. Kuksenok, D. Perchak and A. C. Balazs, *Langmuir*, 2012, **28**, 11410-11421.
20. A. Bera and H. Belhaj, *J. Nat. Gas. Sci. Eng.*, 2016, **34**, 1284-1309.
21. B. Yuan, W. Wang, R. G. Moghanloo, Y. Su, K. Wang and M. Jiang, *Energy & Fuels*, 2016, DOI: 10.1021/acs.energyfuels.6b02108.
22. J. M. Berlin, J. Yu, W. Lu, E. E. Walsh, L. Zhang, P. Zhang, W. Chen, A. T. Kan, M. S. Wong, M. B. Tomson and J. M. Tour, *Energy Environ. Sci.*, 2011, **4**, 505-509.
23. P. C. Mishra, S. Mukherjee, S. K. Nayak and A. Panda, *Inter. Nano. Lett.*, 2014, **4**, 109-120.
24. S. Lim, H. Horiuchi, A. D. Nikolov and D. Wasan, *Langmuir*, 2015, **31**, 5827-5835.
25. A. D. N. Darsh T. Wasan, *Nature*, 2003, **423**, 156-159.
26. K. Kondiparty, A. Nikolov, S. Wu and D. Wasan, *Langmuir*, 2011, **27**, 3324-3335.
27. Z. Hu, S. M. Azmi, G. Raza, P. W. J. Glover and D. Wen, *Energy & Fuels*, 2016, **30**, 2791-2804.
28. A. Esfandyari Bayat, R. Junin, A. Samsuri, A. Piroozian and M. Hokmabadi, *Energy & Fuels*, 2014, **28**, 6255-6266.
29. Y. Zhang, S. Wang, J. Zhou, R. Zhao, G. Benz, S. Tcheimou, J. C. Meredith and S. H. Behrens, *Langmuir*, 2017.
30. H. Zhang, A. Nikolov and D. Wasan, *Langmuir*, 2014, **30**, 9430-9435.
31. H. Wu, J. Chen and H. Liu, *J. Phys. Chem. C.*, 2015, **119**, 13652-13657.
32. J. Zhong, X. Wang, J. Du, L. Wang, Y. Yan and J. Zhang, *J. Phys. Chem. C*, 2013, **117**, 12510-12519.
33. M. Sedghi, M. Piri and L. Goual, *Langmuir*, 2016, 3375-3384.
34. J. Wu, J. He, O. Torsæter and Z. Zhang, presented in part at the SPE International Oilfield Nanotechnology Conference, Noordwijk, The Netherlands, 12-14, June, 2012.
35. K. Yamashita and H. Daiguji, *J. Phys. Chem. C*, 2015, **119**, 3012-3023.
36. E. Oyarzua, J. H. Walther, A. Mejia and H. A. Zambrano, *Phys. Chem. Chem. Phys.*, 2015, **17**, 14731-14739.
37. C. Chen, K. Lu, X. Li, J. Dong, J. Lu and L. Zhuang, *RSC Advances*, 2014, **4**, 6545.
38. C. Bakli and S. Chakraborty, *Soft Matter*, 2015, **11**, 161-168.
39. F. Wang and H. Wu, *Theor. Appl. Mech. Lett.*, 2013, **3**, 054006.

40. X. Wang, S. Xiao, Z. Zhang and J. He, *Energies*, 2017, **10**, 506.
41. S. Supple and N. Quirke, *J. Chem. Phys.*, 2005, **122**, 104706.
42. B. Liu, C. Wang, J. Zhang, S. Xiao, Z. Zhang, Y. Shen, B. Sun and J. He, *Energy & Fuels*, 2017, **31**, 738-746.
43. S. Plimpton, *J. Comput. Phys.*, 1995, **117**, 1-19.
44. H. J. C. Berendsen, J. R. Grigera and T. P. Straatsma, *J. Phys. Chem.*, 1987, **91**, 6269-6271.
45. I. Vorobyov, V. M. Anisimov, S. Greene, R. M. Venable, A. Moser, R. W. Pastor and A. D. MacKerell, *J. Chem. Theory. Compu*, 2007, **3**, 1120-1133.
46. J. G. Harris and K. H. Yung, *J. Phys. Chem.*, 1995, **99**, 12021-12024.
47. S. Xiao, J. He and Z. Zhang, *Nanoscale*, 2016, **8**, 14625-14632.
48. S. Nosé, *Mol. Phys.*, 1984, **52**, 255-268.
49. T. Darden, D. York and L. Pedersen, *J. Chem. Phys.*, 1993, **98**, 10089-10092.
50. W. Humphrey, A. Dalke and K. Schulten, *J. Mol. Graph.*, 1996, **14**, 33-38.
51. J. Xu, Y. Zhang, H. Chen, P. Wang, Z. Xie, Y. Yao, Y. Yan and J. Zhang, *J. Mol. Struct.*, 2013, **1052**, 50-56.
52. J. M. Douillard, *J. Colloid Interface Sci.*, 2009, **337**, 307-310.
53. G. Martic, F. Gentner, D. Seveno, D. Coulon and J. D. Coninck, *Langmuir*, 2002, **18**, 7971-7976.
54. S. Gruener, T. Hofmann, D. Wallacher, A. V. Kityk and P. Huber, *Phys. Rev. E.*, 2009, **79**, 067301.
55. S. Gruener and P. Huber, *Phys. Rev. Lett.*, 2009, **103**, 174501.
56. J. C. Melrose and C. F. Brandner, *J. Can. Petrol.*, 1974, **4**, 54-62.
57. Y. Zhang, S. E. Feller, B. R. Brooks and R. W. Pastor, *J. Chem. Phys.*, 1995, **103**, 10252-10266.
58. F. Leroy, *J. Chem. Phys.*, 2016, **145**, 164705-164716.
59. Y. Yan, X. Wang, Y. Zhang, P. Wang, X. Cao and J. Zhang, *Corros. Sci.*, 2013, **73**, 123-129.

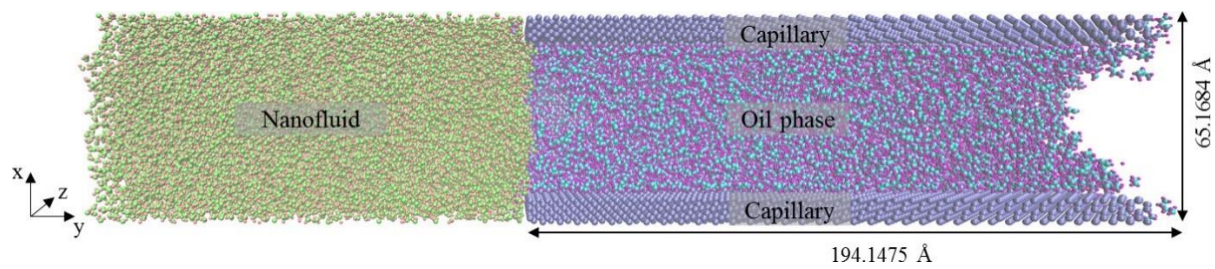


Figure 1. The side view of simulation system containing a water-based nanofluid (green and pink) laden with well-distributed spherical NPs, oil phase (blue and purple) and capillary (purple).

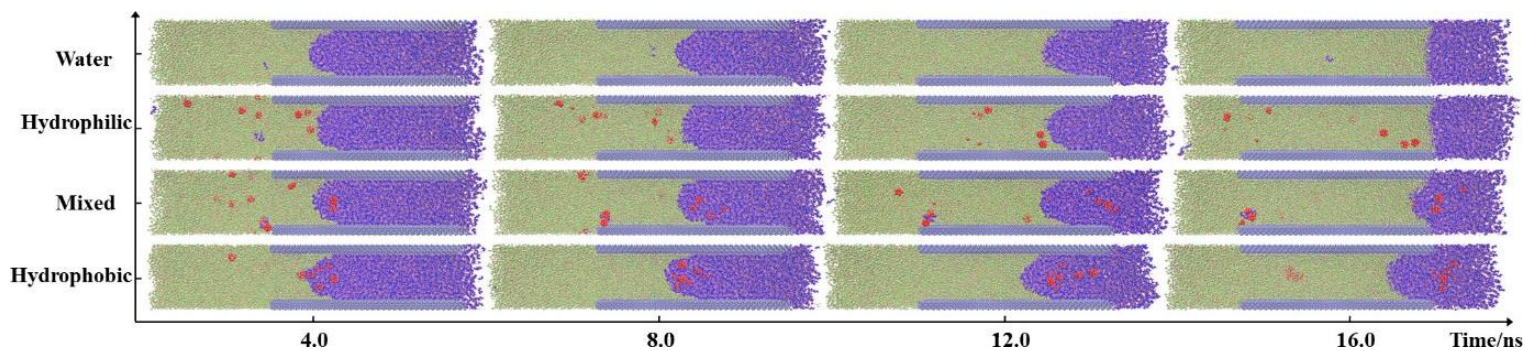


Figure 2. The snapshots of nanofluids displacement with different kinds of NPs. Here, the y-axis shows the wettability properties of NPs and the x-axis is simulation time. The meaning of colors in Figure 2: capillary (blue), water phase (green), oil phase (purple) and NPs (red).

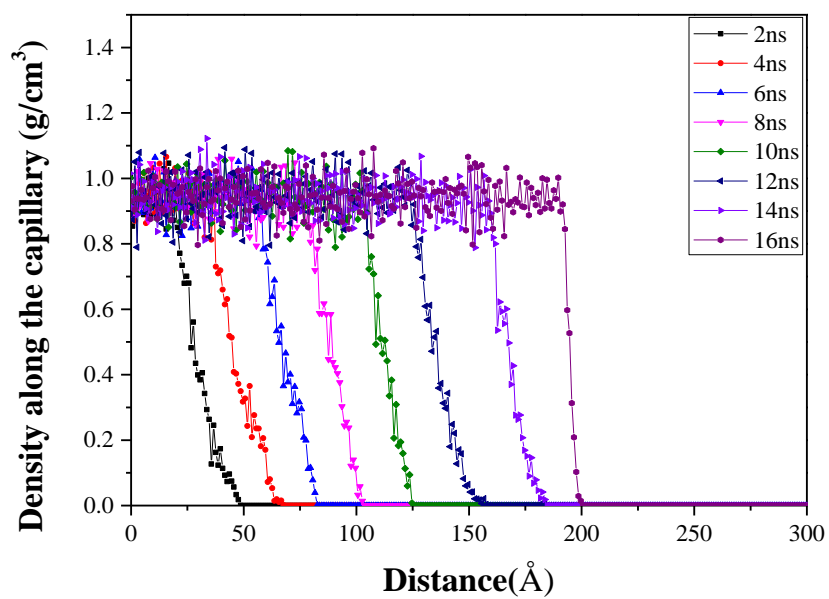


Figure 3. The density distribution profiles of water phase along the capillary. Here, the x axis is the distance from the entrance of the capillary, and the y axis is the density of the fluids.

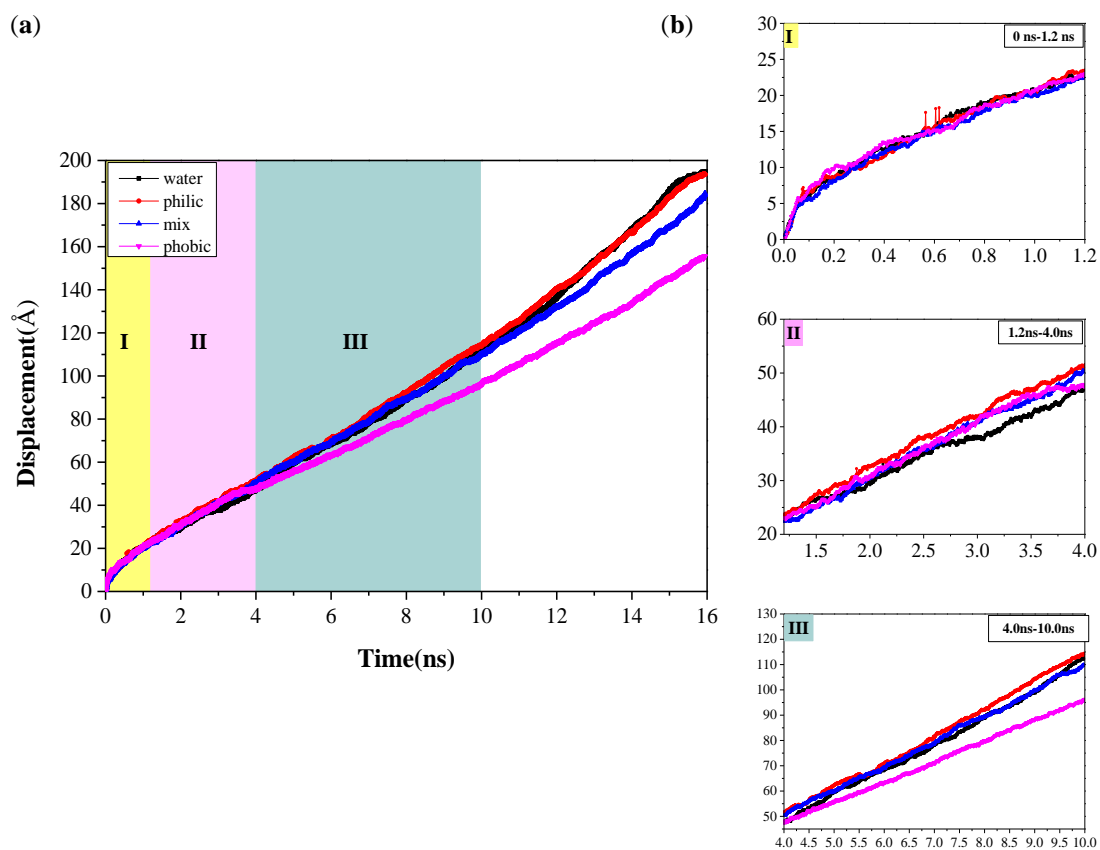


Figure 4. The displacement for nanofluids into the capillary as a function of time. (a) Overall displacement behavior. (b) The enlarged pattern for displacement curves labeled with varied colors in (a) at time: I, 0.0ns-1.2ns; II 1.2ns-4.0ns; III 4.0ns-8.0ns.

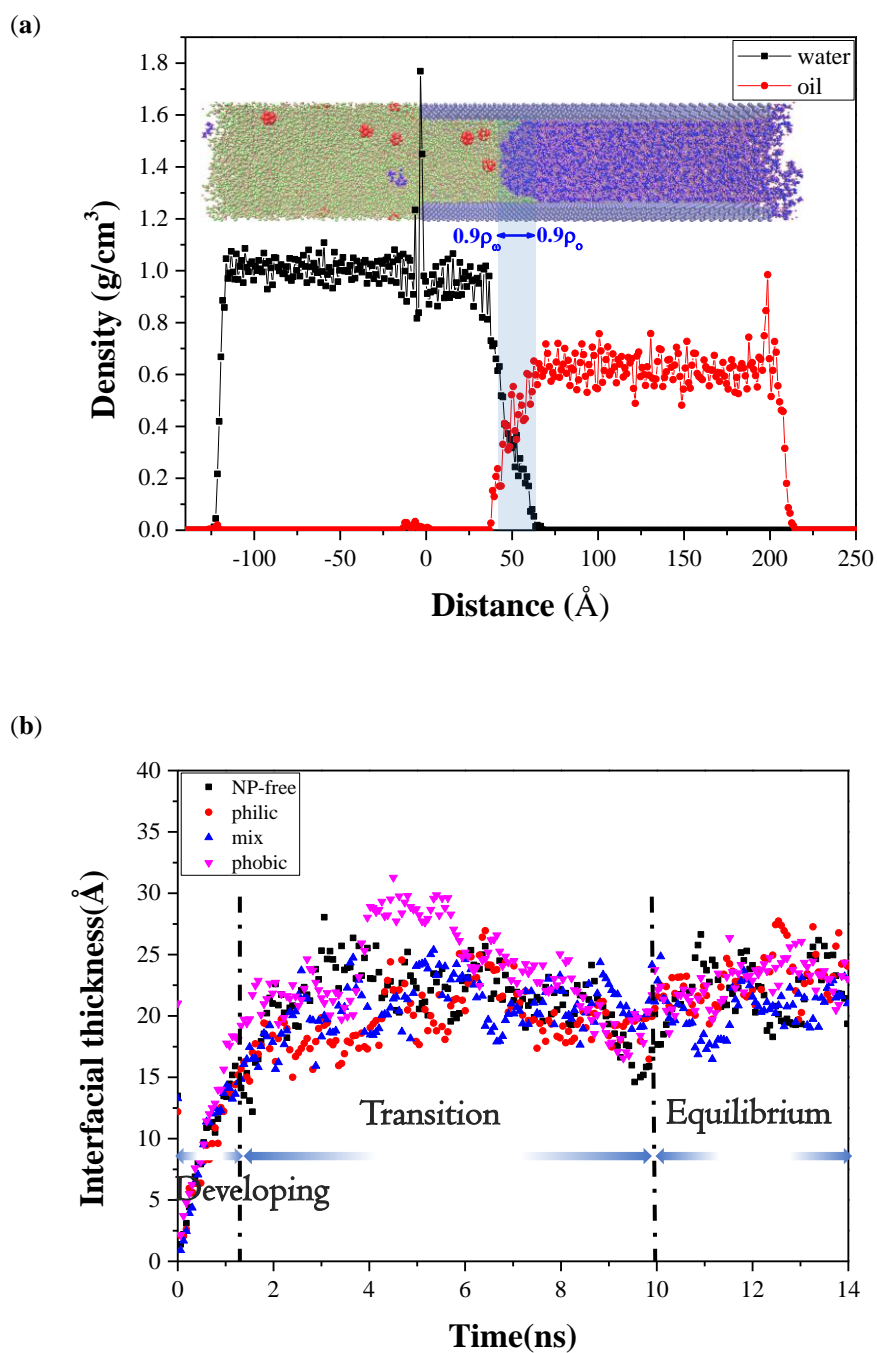


Figure 5. (a) The density distribution profiles of water and oil phase along capillary at 2.0 ns, and the light blue region shows the interfacial thickness region for water-oil fluid; (b) Interfacial thickness evolution.

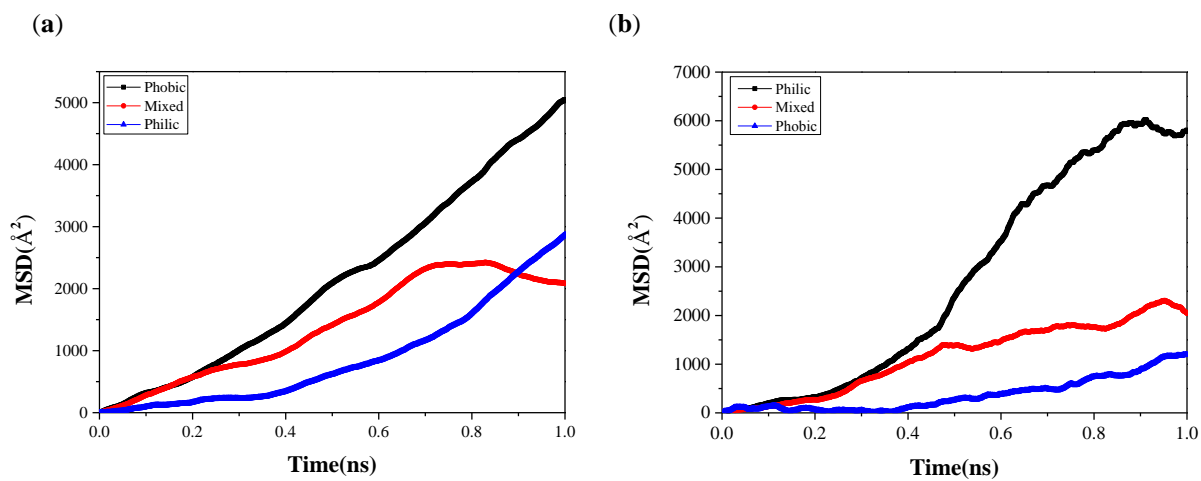


Figure 6. The mean square displacement of water and oil phases with NPs: (a) water phase; (b) oil phase.

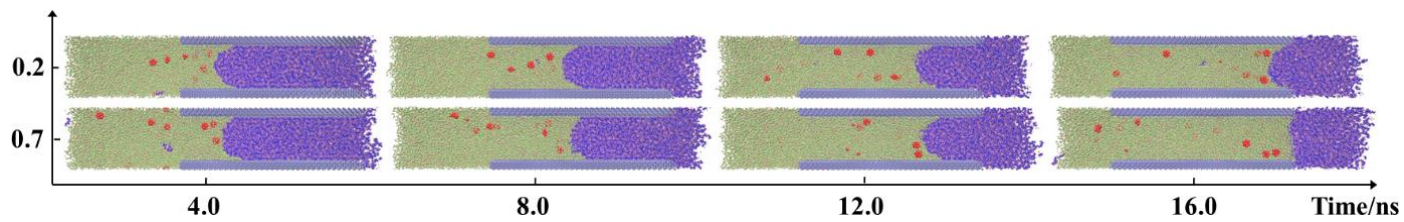
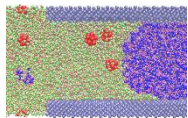
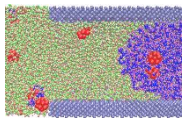
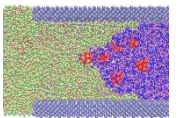


Figure 7. Snapshots of water/oil displacement with hydrophilic NPs possessing different interaction with capillary.

Table 1. The number of NPs behaviors, via, dispersed into fluids, adsorbed on fluids interface and adsorbed on capillary during the displacement process of nanofluids.

Time(ns)	Hydrophilic 			Mixed 			Hydrophobic 		
	water	interface	solid	water	interface	oil	water	interface	oil
2	16	0	0	14	2	0	6/12	2	2
4	16	1	2	12	3	1	5/9	2	5
6	14	1	3	11	1	4	4/9	3	4
8	11	1	4	10	0	5	3/9	1	6
10	12	1	3	9	1	5	2/9	0	7
12	10	2	4	8	1	5	2/9	0	7
14	9	1	6	6	1	6	2/9	0	7

Graphics

